Improving the Utilization of Regenerative Energy and Shaving Power Peaks by Railway Timetable Adjustment

Wang, Pengling; Besinovic, Nikola; Goverde, Rob M.P.; Corman, Francesco

DOI
10.1109/TITS.2022.3145390

Publication date
2022

Document Version
Final published version

Published in
IEEE Transactions on Intelligent Transportation Systems

Improving the Utilization of Regenerative Energy and Shaving Power Peaks by Railway Timetable Adjustment

Wang, Pengling; Besinovic, Nikola; Goverde, Rob M.P.; Corman, Francesco

DOI
10.1109/TITS.2022.3145390

Publication date
2022

Document Version
Accepted author manuscript

Published in
IEEE Transactions on Intelligent Transportation Systems

Improving the Utilization of Regenerative Energy and Shaving Power Peaks by Railway Timetable Adjustment

Pengling Wang, Nikola Bešinović, Rob M. P. Goverde, *Member, IEEE*, and Francesco Corman, *Member, IEEE*

***Abstract*— Employing regenerative braking in trains contributes to reducing the amount of energy used, especially when applied to commuter trains and to those used on very dense suburban networks. This paper presents a method to fine-tune the periodic timetable to improve the utilization of regenerative energy and to shave power peaks while maintaining the structure and robustness of the original timetable. First, a mixed-integer linear programming model based on the periodic event scheduling framework is proposed. A set of feasible timetables is determined and optimized with the aim of increasing synchronized acceleration and braking events at the same station, and maintaining the timetable robustness at the specified level. Next, a local search algorithm is developed to optimize the timetable such that the power peak value is minimized. The max-plus system model is adopted to estimate the delay propagation. Monte Carlo simulation is used to evaluate the utilization of regenerative energy and power peaks in random delayed circumstances. The proposed method was adopted to fine-tune the 2019 timetable for a sub-network of the Dutch railway. In the case of on-time scenarios, the optimized timetable increases the regenerative energy usage by almost 290% and decreases the 15-minute power peaks by 8.5%. In the case of delay scenarios, the optimized timetable outperforms the original timetable in terms of using regenerative energy and shaving power peaks.**

***Index Terms*— Railway timetabling, utilization of regenerative energy, power peak shaving.**

I. Introduction

RAIL is among the most energy-efficient modes of transport for freight and passengers, but increasing the energy efficiency and thus saving energy still plays a key role in modern railway companies' strategies. In fact, rail operators are under enormous pressure as a result of societal and environmental targets to increase the sustainability of railway transportation. Consequently, energy efficiency has emerged as a prominent subject in railway operations in both industry and academia.

Improving the energy efficiency of train operations is not simply a matter of minimizing the energy requirements for traction, but also of shaving power peaks. This topic is of particular importance in DC systems with non-inverting substations. Here, energy billing is often determined by two components: total energy consumption and power peaks. For example, the German railway operator DB, via its subsidiary DB Energie, charges train operators according to both the total energy consumption and the maximum power consumption of the trains they operate. In terms of the total consumption, they pay a certain price per kilowatt-hour to which federal fees and an apportionment are added. The second component is based on the maximum peak power consumption of all trains over a 15-minute interval during the billing period. This amount is calculated by summing up the energy consumption of all trains and then averaging this value over the four 15-minute clock intervals. The train operators then pay a certain rate per kilowatt, which is multiplied by the highest average value [1], [2].

The effective use of regenerative energy can contribute directly to a reduction in the amount of energy to be purchased. In general, several types of train braking systems exist, including regenerative braking, resistance braking, and air braking. During regenerative braking, which is commonly employed in current electric rail systems, a train decelerates by reversing the functioning of its motors. These motors then act as generators that convert mechanical energy into electrical energy that can be either used immediately or stored until needed [3]. In this paper, the electrical energy produced in this way is referred to as "regenerative energy". The regenerative energy primarily feeds the auxiliary functions of the vehicle, and the excess energy is usually returned to the supply line to power other trains accelerating along the same electric section. However, because the auxiliaries consume a relatively minor amount of energy and different trains are unlikely to simultaneously accelerate and decelerate, a considerable amount of braking energy is wasted. In fact, many countries

Manuscript received December 22, 2020; revised June 27, 2021, October 6, 2021, and December 7, 2021; accepted January 19, 2022. This work was supported in part by the Fundamental Research Funds for the Central Universities, in part by the Shanghai Sailing Program under Grant 21YF1450200, in part by the National Natural Science Foundation of China under Grant 72101184, in part by the Swiss National Science Foundation under Project 181210/DADA, in part by the Swiss Innovation Agency Innosuisse, and in part by the Swiss Competence Center for Energy Research—SCCER Mobility. The Associate Editor for this article was H. B. Celikoglu. *(Corresponding author: Pengling Wang.)*

Pengling Wang is with the College of Transportation Engineering, Tongji University, Shanghai 200070, China, and also with the Institute for Transport Planning and Systems, Swiss Federal Institute of Technology, ETH Zürich, 8092 Zürich, Switzerland (e-mail: pengling_wang@tongji.edu.cn).

Nikola Bešinović and Rob M. P. Goverde are with the Department of Transport and Planning, Delft University of Technology, 2628 CD Delft, The Netherlands.

Francesco Corman is with the Institute for Transport Planning and Systems, Swiss Federal Institute of Technology, ETH Zürich, 8092 Zürich, Switzerland.

Digital Object Identifier 10.1109/TITS.2022.3145390

use timetables that allow multiple trains to simultaneously accelerate on the network at the same time. Consequently, during these phases, the power requirement in the traction network increases significantly. In addition, the increasing volume of traffic and use of more powerful trains causes the maximum power requirement to increase.

Synchronizing accelerating and braking trains by means of timetable optimization would be a straightforward way to increase the use of regenerative braking energy. Additionally, it may limit power peaks and stabilize the power voltage because more accelerating trains would draw power from braking trains, instead of from the power system. This motivated us to study the energy-efficient timetable optimization problem with the aim of maximizing the utilization of regenerative energy and shaving power peaks. We focused on the passenger-train periodic timetable used for the Dutch railway network, which carries dense traffic, has metro-like operations, relies on balanced train flows in both directions, and is powered by a DC power grid system.

II. Literature Review

The energy-efficient timetabling problem focuses on seeking the optimal arrival and departure times of trains to improve the energy efficiency of railway operations [4], [5]. This section presents a literature review of those studies with a specific focus on improving the utilization of regenerative braking energy by timetable optimization.

A. Pure Timetable Optimization

Early research was concerned with dwell time control [6] and run time control [1] to achieve synchronized acceleration and braking processes for the utilization of regenerative energy. Subsequent work [7] led to the proposal of a timetable adjustment model to maximize the time during which the accelerating and braking actions of trains overlap within the same substation. This work was extended [8] to synchronize the braking and acceleration processes of all trains traveling along the same electrical section. They developed a power flow model to calculate the regenerative saving factor each time these two processes were synchronized within an electrical section. However, the specific speed profiles of trains were not considered, and the acceleration and braking processes were described as a fixed duration. Other researchers [9] coordinated the accelerating and braking processes of adjacent trains by adjusting the headway and dwell times. This work was extended [10] by including random departure delays at busy stations to increase synchronizations. Another approach [11] involved the adoption of real-world speed profiles for energy estimation and led to the proposal of a dwell time control approach for minimizing the net energy (traction energy minus regenerative energy) of all trains located in the same electricity supply interval. Similarly in [12], a headway and dwell time adjustment model was presented with the aim of maximizing the utilization of regenerative energy. The proposed model was solved using an improved artificial bee colony algorithm. In this regard, [13] considered passenger convenience and built a bi-objective timetable optimization model and a GA-based solution method to find the optimal timetable with the minimum passenger waiting time and net energy consumption. Another study resulted in the proposal of a mixed integer linear programming (MILP) model for feasible adaptations of the German timetable draft. The performance of this model was investigated under different objective functions: reducing the energy cost and increasing the stability of the power supply system (reducing power peaks). However, the models used in this study are not yet able to solve instances of the relevant size [2], [14].

B. Integrated Optimization of Timetable and Speed Profile

Utilizing regenerative energy relies on the coordination of the movements of neighboring trains [15]–[17]. A possible approach would be to improve the usage of regenerative energy by simultaneously optimizing train timetabling and speed profiles [18]–[27].

Specifically, references [18]–[20] investigated the problem of optimizing the integration of energy-efficient driving and timetable design for a railway corridor with one type of cyclic train operation. A method for departure time adjustment was proposed to increase the synchronized braking and acceleration processes for the utilization of regenerative braking. Others proposed an integrated optimization model for metro lines [21], [22]. The model adopts the switching times and speeds of the train control regimes (acceleration, cruising, coasting, and braking) as the decision variables, aims to minimize the net energy consumption of multiple trains, and considers the constraints with respect to the number of trains, cycle times, switching times, turnaround times, vehicle speed limits, and dwell times. Another study [23] considered the passenger waiting times and proposed an integrated optimization model to coordinate trains at the same station to improve the utilization of regenerative energy and decrease passenger's waiting time. More recently, the energy-efficient driving problem was incorporated into the railway timetabling process based on a space-time-speed (STC) network [24], [25]. The STC grid network was constructed for joint train routing, timetabling, and trajectory optimization as a path-finding problem. In addition, a set of energy-efficient speed trajectories was predefined. Based on these speed trajectories, a near-optimal energy-efficient timetable solution with dynamic headways was found using a heuristic algorithm.

C. Focus of This Study

As summarized in Table I, despite the various insights provided by manipulating the running times, dwell times, headway times, and driving strategies to synchronize accelerating and braking trains with the intention of maximizing the reuse of regenerative energy, we noticed the following significant knowledge gaps:

1. Past studies on energy-efficient timetabling for the utilization of regenerative energy mainly focused on non-periodic timetables for a corridor and cyclic timetables for metro systems, where a single type of train operates solely in each corridor. Research involving periodic timetables of mainline rail networks is rarely reported. This is because the traffic

TABLE I
SUMMARY OF MOST RELEVANT REFERENCES

Publication	Research object	Usage of regenerative energy	Power peak shaving	Delay impact
Ramos et al. [7] Peña-Alcaraz et al. [8]	A metro line with one type of cyclic train operation	An ILP model for improving overlapping times of synchronized acceleration and braking processes	None	None
Yang et al. [9, 11]; Li and Yang [10]	A metro line with one type of cyclic train operation	An ILP model with real-world speed profiles to minimize the energy costs	None	Random departure delays are adopted to increase the synchronization of acceleration and braking processes
Sun et al. [13]	A metro line with one type of cyclic train operation	Timetable optimization for the usage of regenerative energy and passenger waiting time	None	None
Bärmann et al. [2, 14]	Non-periodic timetable for mainlines	MILP model for improving the usage of regenerative energy	Minimize the 15 - minutes power peak	None
Su et al. [18, 19, 20]	A metro line with one type of cyclic train operation	Jointly optimize timetables and speed profiles; a method that adjusts the departure time to increase synchronized braking and acceleration processes	None	None
Li and Lo [21, 22]	A metro line with one type of cyclic train operation	jointly optimize timetables and speed profiles to minimize net energy consumption	None	None
Yang et al. [23]	A metro line with one type of cyclic train operation	ILP model for joint design of energy-efficient timetables and speed profiles	None	None
Zhou et al. [24] Xu et al. [25]	Non-periodic timetable for a high-speed railway corridor	STC grid networks for joint design of energy-efficient timetables and speed profiles	None	None
This paper	Periodic timetable for mainlines	MILP model for improving overlapping times of synchronized acceleration and braking processes and maintaining the timetable robustness level	A local search algorithm for shaving power demand peaks	Monte Carlo simulation for a max-plus linear system is constructed to estimate the impact of delays

situation on these networks is much more complex, as different types of trains operate alternatively along each corridor, with the result that a greater variety of trains may interact with each other along the same corridor.

2. Adjusting the running/dwell/headway times for the utilization of regenerative energy changes the time allowance distribution and affects the robustness of the timetable. Few reports on ways to improve the energy efficiency without negatively impacting upon the robustness of the timetable have been published.

3. Synchronizing accelerating and braking trains may limit peaks in the power consumption and stabilize the power voltage. In fact, high-power peaks are mainly caused by the fact that more than one train accelerates at the same time. Accelerating trains that draw power from braking trains, instead of from the power system, would reduce the demand for power. However, synchronizing the accelerating and braking processes does not directly reduce simultaneous accelerations. In other words, enhancing the benefits of power peak shaving would require additional measures. Unfortunately, few recent attempts to solve the timetabling problem to enhance these benefits have been reported. To the best of our knowledge, only one research group [2], [14] conducted a few studies related to this topic.

4. Finally, much research has focused on the planning phase; the impact of delays on the usage of regenerative energy and the power peaks remains unknown.

This study aims to fill these knowledge gaps by proposing a periodic timetable adjustment method with the objective of increasing the utilization of regenerative energy and shaving power peaks while maintaining the robustness of the timetable at the required level. This entailed the use of Monte Carlo simulation for a max-plus linear system to estimate the impact of delays on the energy costs and power peaks.

The proposed periodic timetable adjustment model was built on the basis of the basic framework of the periodic event scheduling problem (PESP) [28]. Our approach was to focus on adjusting existing timetables, instead of building completely new ones, to enhance the usage of regenerative energy while maintaining the structure (e.g., train orders and periodicity) of existing timetables and ensuring the same level of service to passengers as in existing timetables. Moreover, timetable adjustment has less impact on the scheduling of rolling stock and crew compared to the construction of new timetables.

The proposed timetable adjustment model maximizes the times at which the synchronized acceleration and braking processes overlap at the same station as the main objective and maintains the timetable robustness as an ε-constraint. Thus far, strong consensus on the meaning of robustness does not exist. Researchers often evaluate timetable robustness with the value of time allowances inserted in the timetable [29]. Here, the time allowances are partitioned in the time supplements (or time allowances) on top of the minimum process times

(running/dwell times), and the buffer times on top of the minimum headway times. Timetable robustness is improved by increasing the time allowances or ensuring they are well distributed [30]. A parameter θ, which is introduced to quantify the timetable robustness level, is computed as the sum of the weighted time allowances in the running times, dwell times, and headway times. The larger θ is, the larger the time allowances are, and therefore, the more robust the timetable is against delays.

The power peak shaving method we built first integrates the energy-efficient train trajectory optimization model to find energy-efficient driving strategies) with the corresponding power profiles of every possible train run. Then, based on these power profiles, the overall power profiles are computed for different timetables. A power peak shaving algorithm was developed to search for the local optimal timetable with a minimal power peak. Note that the power peak we discuss here refers to the maximum traction power demand of all trains in a railway network over a certain time period, instead of the power peak that occurs in the electrical system of the railway network. We use the maximum traction power demand as the power peak because the price paid for energy in many countries is partially determined by the peak in the power demand (see Section I). A case study was designed by applying the proposed timetable adjustment model and power peak shaving algorithm to fine-tune the timetable of 2019 for a sub-network of the Dutch railway. To examine how the timetable adapts to uncertain delays, the max-plus theory [31] was adopted to estimate the delay propagation. Monte Carlo simulation was used to evaluate the utilization of regenerative energy and power peaks during random delays.

To summarize, the contributions of this study to the literature on energy-efficient timetabling are as follows.

1. A timetable adjustment model was proposed to fine-tune a periodic timetable for the utilization of regenerative energy. Compared to the existing literature on cyclic timetables in metro lines or non-periodic timetables in a single corridor, our work considers a more complex traffic situation in a mainline network and periodic timetables.

2. The timetable adjustment takes into account the requests to ensure timetable robustness and enhance the benefit of power peak shaving. The proposed timetable adjustment model maximizes the times during which synchronized acceleration and braking processes overlap as the main objective and maintains the timetable robustness as an ε-constraint. A local search algorithm is built to enhance the benefit of using the optimized timetable for smoothing the power demand profile.

3. The max-plus theory was adopted to estimate delay propagation. A model based on Monte Carlo simulation was constructed to evaluate the timetable robustness, energy efficiency, and power peaks when delays occur. The simulation results show that even in the case of delays, the optimized timetable outperforms the original timetable in terms of recovering from delays by using regenerative energy and shaving power peaks.

The remainder of this paper is organized as follows. In Sections III and IV, we discuss our energy-efficient timetable optimization model and power peak shaving algorithm, respectively. In Section V, we present the max-plus theory we use to consider delayed operations. In Section VI, the performance of the proposed optimization method is evaluated using real-life instances. In Section VII, we draw conclusions and discuss future research directions.

III. Energy-Efficient Timetabling

This section presents the PESP-based timetable adjustment model that aims to adjust the arrival and departure times of a given timetable to increase the occurrence of synchronized acceleration and braking processes while maintaining the timetable robustness at a certain level.

A. Basic PESP Model

The PESP model schedules events in a period of the cyclic timetable and considers precedence constraints and relations between events. The PESP formulation can be represented by a directed graph $G = (E, A)$. The set E represents train events such as arrivals at, departures from, and passing through stations and important timetabling locations (i.e., bridges and junctions). These events are linked by the set of activities A, representing the constraints on the timing between a pair of events. In this study, the activity set A is equal to $A_{\text{run}} \cup A_{\text{dwell}} \cup A_{\text{headway}} \cup A_{\text{transfer}} \cup A_{\text{turn}} \cup A_{\text{sab}}$. A_{run} denotes the set of running activities. A running activity represents the running time constraint between two successive departure and arrival events of a train. A_{dwell} is the set of dwell activities. A dwell activity represents the dwell time constraint between an arrival event and a departure event of a train at a station. A_{headway} is the set of headway activities. A headway activity refers to the headway time constraint between two successive trains traveling on the same lines at stations. A_{transfer} is the set of transfer connection activities. A transfer connection activity represents the transfer time constraint for passengers transferring from an arriving train (an arrival event) to a departing train (a departure event of another train) at a station. A_{turn} is the set of turnaround activities. A turnaround activity refers to the time constraint between the arrival of a train at its end station and the departure of the train (typically the same rolling stock, but a different service number) from the opposite line that leaves from that station. A_{sab} is the set of activities with synchronized acceleration and braking events. An activity $(i, j) \in A_{\text{sab}}$ refers to the overlap time of departure event i and arrival event j. The synchronization pair may occur within one station or one electrical section, depending on the needs of the model. If the model is designed to employ synchronization pairs within the same station, it is assumed that trains in the same station are powered by the same electrical section.

The periodic train timetabling problem then determines the discrete times π_i associated with each event i of E without violating the set of constraints A. These events repeat every cycle at time instances $\pi_i + kT$, where $k = 1, 2, \ldots$. As the problem is to define the events within an interval of cycle time T, π_i is restricted to the interval $[0, T - 1]$. A pair of events can be realized in two different orders while maintaining their event times within the interval $[0, T - 1]$. The PESP constraints can then be

TABLE II
DETERMINATION OF OVERLAPPING TIME

Case	Sequence	Overlapping time	
		(a)	(b)
1	$\pi_i, \pi_j^-, \pi_j, \pi_i^+$	t_j	t_j
2	$\pi_j^-, \pi_i, \pi_i^+, \pi_j$	t_i	t_i
3	$\pi_i, \pi_j^-, \pi_i^+, \pi_j$	$\pi_i - \pi_j + t_i + t_j$	$\pi_i - \pi_j - T + t_i + t_j$
4	$\pi_j^-, \pi_i, \pi_j, \pi_i^+$	$\pi_j - \pi_i$	$\pi_j - \pi_i + T$
5	$\pi_i, \pi_i^+, \pi_j^-, \pi_j$	0	0
6	$\pi_j^-, \pi_j, \pi_i, \pi_i^+$	0	0

formulated mathematically as

$$\underline{\mu}_{ij} \le \pi_j - \pi_i + q_{ij}T \le \overline{\mu}_{ij}, \quad \forall (i,j) \in \overline{A}, \tag{1}$$

$$0 \le \pi_i \le T-1, \quad \forall i \in E, \tag{2}$$

$$q_{ij} \ge 0, \quad \forall (i,j) \in \overline{A}, \tag{3}$$

$$q_{ij} + q_{i'j'} + q_{ii'} + q_{jj'} = 2o_{ii'jj'}, \quad \forall (i,j),(i',j') \in A_{\text{run}}, (i,i'),(j,j') \in A_{\text{headway}}, \tag{4}$$

$$0 \le o_{ii'jj'} \le 2, \quad \forall (i,j),(i',j') \in A_{\text{run}}, (i,i'),(j,j') \in A_{\text{headway}}. \tag{5}$$

where $\overline{A} = A_{\text{run}} \cup A_{\text{dwell}} \cup A_{\text{headway}} \cup A_{\text{transfer}} \cup A_{\text{turn}}$. Constraint (1) ensures that all activities are within the given bounds, $\underline{\mu}_{ij}$ and $\overline{\mu}_{ij} \in [0, T-1]$. It consists of restrictions on running times, dwell times, headway times, transfer connecting times, and turn-around times. Constraint (2) requires the periodicity of events by bounding to $[0, T-1]$. Constraint (3) restricts q_{ij} to non-negative integers, representing the number of crossed time periods of event j compared to event i. If i and j take place in the same period, $q_{ij} = 0$; in the case that j takes place in the next period of i, $q_{ij} = 1$, and so on. Constraints (4-5) guarantee that no illegal overtaking can arise, by restricting the sum of the four binary parameters of related running and headway activities to 0, 2, or 4 [32], where $o_{ii'jj'}$ is a dummy integer to avoid illegal overtakes, $o_{ii'jj'} \in \{0, 1, 2\}$.

B. Synchronization of Acceleration and Braking Processes

The power recovered via regenerative braking can be used if the power is simultaneously drawn from somewhere close. Taking an activity $(i, j) \in A_{\text{sab}}$ (i and j are departure and arrival events, respectively) as an example, Table II presents six possible combinations of synchronizations and their overlapping times [8]. The third column in Table II (overlapping time (a)) reports the overlapping times when the four events $(\pi_i, \pi_j^-, \pi_j, \pi_i^+)$ take place in one period, while the fourth column (overlapping time (b)) reports the overlapping times when the four events occur across two time periods. π_i is the time of departure event i, π_j is the time of arrival event j, and t_i and t_j are the acceleration time after event i and the braking time before event j, respectively. $\pi_i^+ = \pi_i + t_i$ denotes the end time of the acceleration process. $\pi_j^- = \pi_j - t_j$ is the start time of the braking process. It is assumed that t_i and t_j are independent of π_i and π_j, respectively. In addition, $t_i, t_j \ll T$, meaning that the braking and acceleration times are much smaller than the time period T; thus, the overlapping time of $(i, j) \in A^{\text{sab}}$ is much smaller than T.

In Table II, the acceleration and braking processes are (at least partially) synchronized in Case 1-4, where the overlapping times are computed differently according to the sequence of π_i, π_i^+, π_j^-, and π_j. Because event i may take place before or after j in one time period, the order of events affects the computation of overlapping times (see Cases 3 (a)–(b) and 4 (a)–(b) in Table II). For all activities within A_{sab} ($\forall (i, j) \in A_{\text{sab}}$), two binary variables, α_{ij} and β_{ij}, are introduced to indicate whether events i and j are synchronized.

$$\alpha_{ij} = \begin{cases} 1, \text{ if } \pi_j \ge \pi_i, \pi_i + t_i \ge \pi_j - t_j, \\ 0, \qquad \text{otherwise.} \end{cases} \tag{6}$$

$$\beta_{ij} = \begin{cases} 1, \text{ if } \pi_j + T \ge \pi_i, \pi_i + t_i \ge \pi_j - t_j + T, \\ 0, \qquad \text{otherwise.} \end{cases} \tag{7}$$

where $\alpha_{ij} = 1$ refers to the synchronized cases if $\pi_i \le \pi_j$, $\beta_{ij} = 1$ refers to the synchronized cases if $\pi_i > \pi_j$, and $\alpha_{ij} + \beta_{ij} \le 1$. Together with the two binary variables and the methods for calculating the overlapping time presented in Table II, we formulate the objective and constraints for maximizing the total overlapping times as follows:

$$\max \sum_{\forall (i,j) \in A_{\text{sab}}} L_{ij}, \tag{8}$$

$$\text{s.t.} \quad L'_{ij} = \min\{\pi_j - \pi_i + \beta_{ij}T, \pi_i - \pi_j - \beta_{ij}T + t_j + t_i, t_j, t_i\}, \tag{9}$$

$$M \cdot (\alpha_{ij} + \beta_{ij} - 1) \le L_{ij} - L'_{ij} \le -M \cdot (\alpha_{ij} + \beta_{ij} - 1), \tag{10}$$

$$-M \cdot (\alpha_{ij} + \beta_{ij}) \le L_{ij} \le M \cdot (\alpha_{ij} + \beta_{ij}), \tag{11}$$

$$\alpha_{ij} \ge \min\left\{\frac{\pi_j - \pi_i}{M}, \frac{\pi_i - \pi_j + t_i + t_j}{M}\right\}, \tag{12}$$

$$\alpha_{ij} \le 1 + \min\left\{\frac{\pi_j - \pi_i}{M}, \frac{\pi_i - \pi_j + t_i + t_j}{M}\right\}, \tag{13}$$

$$\beta_{ij} \ge \min\left\{\frac{\pi_j - \pi_i + T}{M}, \frac{\pi_i - \pi_j - T + t_i + t_j}{M}\right\}, \tag{14}$$

$$\beta_{ij} \le 1 + \min\left\{\frac{\pi_j - \pi_i + T}{M}, \frac{\pi_i - \pi_j - T + t_i + t_j}{M}\right\}, \tag{15}$$

$$\alpha_{ij}, \beta_{ij} \in \{0, 1\}, \quad \forall (i, j) \in A_{\text{sab}}. \tag{16}$$

where L_{ij} refers to the overlapping time of events j and i. M is a large positive integer. The objective function (8) aims to maximize the total overlapping times of the synchronized acceleration and braking processes. Constraint (9) introduces an integer value L'_{ij}, which models the overlapping time of events i and j when the two events are synchronized. Constraints (10-11) force $L_{ij} = L'_{ij}$ in the case that $\alpha_{ij} + \beta_{ij} = 1$, otherwise $L_{ij} = 0$. Constraints (12)–(15) are the linearized versions of Equations (6)–(7). Constraint (16) restricts α_{ij}, β_{ij} to be binary variables.

C. Additional Constraints for Fine-Tuning and Robustness

This model is designed to fine-tune the given timetables. We enforce the fine-tuning changes such that they have a

minor effect on the structure of the timetable by means of the constraints:

$$\underline{c} \le \pi_i - \pi_i^* + g_i T \le \overline{c}, \quad \forall i \in E, \tag{17}$$

$$-1 \le g_i \le 1, \quad \forall i \in E, \tag{18}$$

where π_i^* refers to the time of event i in the given timetable, and $\underline{c}$ and $\overline{c}$ are the minimum and maximum allowed changes, respectively. Further, $g_i \in [-1, 1]$ are integers. $g_i = 0$ if π_i and π_i^* are in the same period, $g_i = 1$ if π_i is in the next period of π_i^*, and $g_i = -1$ if π_i is in the previous period of π_i^*.

This work balances the robustness and energy efficiency by considering the improvement of synchronized acceleration and braking processes as the main objective while maintaining robustness as an ε constraint. As discussed in Section II, the time allowances inside a timetable are adopted to represent timetable robustness. A parameter θ is introduced to quantify the timetable robustness level:

$$\begin{aligned}\theta = \gamma_1 \cdot \sum_{(i,j)\in A_{\text{run}}} (\pi_j - \pi_i + q_{ij}T - \underline{\mu}_{ij}) \\ + \gamma_2 \cdot \sum_{(i,j)\in A_{\text{dwell}}} (\pi_j - \pi_i + q_{ij}T - \underline{\mu}_{ij}) \\ + \gamma_3 \cdot \sum_{(i,j)\in A_{\text{headway}}} (\pi_j - \pi_i + q_{ij}T - \underline{\mu}_{ij}),\end{aligned} \tag{19}$$

where γ_1, γ_2, and γ_3 are the weight factors and θ is the sum of the weighted time allowances in the running times, dwell times, and headway times. The time allowances are beneficial for absorbing small delays and reducing the delay propagation. A larger θ indicates improved timetable robustness. To ensure the robustness of the optimized timetable, a lower bound restricts the total weighted time allowance θ:

$$\theta \ge \varepsilon, \tag{20}$$

where ε is a constant value, that is, the minimum acceptable robustness level (total weighted time allowances). Moreover, we wish to include at least some time allowances in all activities by restricting

$$\pi_j - \pi_i + q_{ij}T - \underline{\mu}_{ij} \ge \chi_{ij}, \quad \forall (i,j) \in A_{\text{run}} \cup A_{\text{dwell}} \cup A_{\text{headway}}, \tag{21}$$

where χ_{ij} is a constant value, referring to the minimum time allowance requested in an activity $(i, j) \in A_{\text{run}} \cup A_{\text{dwell}} \cup A_{\text{headway}}$. In summary, the timetable adjustment model aims to maximize the objective functions (8) subject to constraints (1–5 and 9–21).

IV. Power Peak Shaving

The timetable adjustment model presented in Section III produces optimal solutions in terms of the maximal overlapping time of acceleration and braking processes. These optimal solutions may contribute to smooth power consumption profiles. This section presents the algorithm that ensures that power peak shaving benefits from the optimized timetable.

As the cost of energy is directly related to the total power demand of the trains, the proposed power peak shaving algorithm focuses on minimizing the power demand peaks resulting from traction, instead of minimizing the power peaks measured from the overhead lines. That is, the electrical system was not considered in this work. To calculate the power demand profile of all involved trains, we first compute the power profile of every train with an energy-efficient train trajectory optimization model considering the regenerative energy (Section IV-A). The method for the calculation of the power profile of all involved trains is presented in Section IV-B, and the algorithm for power peak shaving is introduced in Section IV-C. To emphasize that multiple timetables are used, a superscript ψ is added to the timetable-related variables.

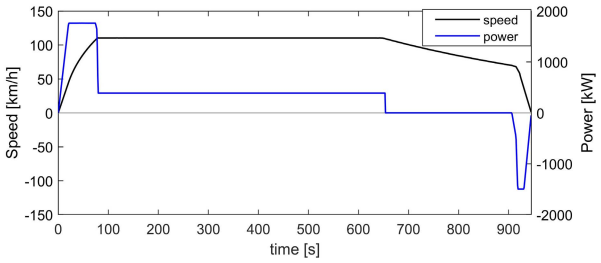

Fig. 1. Speed (black) and power (blue) consumption profile of an intercity train on an even track.

A. Single Train Power Profile

Taking a train run between event i (departure event) and j (arrival event) within a given run time r as an example, we compute the speed profile and power profile for any combination of (i, j, r) with the multiple-phase optimal control (MPOC) method [33]. This MPOC method optimizes the sequence of train control regimes with the objective of minimizing the traction energy costs subject to the timetable constraints, maximum speed restrictions, maximum power/force restrictions, etc. This study extends the objective function to include the reuse of regenerative energy, whereas the remainder of the MPOC model remains the same as before [33]. The typical speed and power profile of a train running on an even track are shown in Fig. 1.

Using the MPOC method, we compute the power profiles of every possible train run (different combinations of arrival/departure events and running times) in advance. These power profiles were used as inputs for the power peak shaving model presented below.

B. Power Peak Shaving Model

First, to compute the power profiles of all trains, it is necessary to assess the total power consumption every second (or a similar small time interval). We discretize the time period as $0, \delta, 2\delta, \ldots, T - \delta$, where T is the period of the timetable, and δ is the discrete time interval (e.g., 1 s). We denote $\Omega = [0, \delta, 2\delta, \ldots, T - \delta]$ as the set of discretized timestamps, and $t \in \Omega$ is a timestamp within Ω. The power consumption at every timestamp is calculated as the sum of the demanded and regenerative power of all trains.

We pre-calculate the power profiles of every train run using the method outlined above (Section IV-A). The power profile of a single train run is expressed as

$$P^{ijr} = [p_0^{ijr}, p_\delta^{ijr}, p_{2\delta}^{ijr}, \ldots, p_{h\delta}^{ijr}, \ldots], \tag{22}$$

where $(i, j) \in A_{\text{run}}^{\psi}$ (A_{run}^{ψ} is the set of running activities with timetable ψ), r denotes the running time between i (departure event) and j (arrival event), and $p_{h\delta}^{ijr}$ refers to the power consumption at time $h\delta + \pi_i^{\psi}$ (π_i^{ψ} refers to the scheduled time of event i with timetable ψ).

Constructing the power profile of all involved trains requires knowledge of the power demand of every train run $(i, j) \in A_{\text{run}}^{\psi}$ at every timestamp t. Furthermore, to obtain the power consumption of a train run (i, j) at timestamp t, we need to know the running time after departure event i at timestamp t, which is calculated as

$$\eta_{ijt}^{\psi} = \begin{cases} t - \pi_i^{\psi} & \text{if} \quad \pi_i^{\psi} \le t \le \pi_j^{\psi} + q_{ij}^{\psi} T, \\ t - \pi_i^{\psi} + T & \text{if} \quad t \le \pi_j^{\psi} < \pi_i^{\psi}, \\ 0 & \text{otherwise.} \end{cases} \tag{23}$$

where $(i, j) \in A_{\text{run}}^{\psi}, t \in \Omega$, η_{ijt}^{ψ} represents the running time after event i in the timetable ψ at timestamp t, and η_{ijt}^{ψ} is calculated differently depending on whether departure event i takes place before or after arrival event j in one time period. We denote by p_{ijt}^{ψ} the power demand of a train run (i, j) at timestamp t, which is computed as

$$p_{ijt}^{\psi} = \begin{cases} p_{h\delta}^{ijr}, & \text{if} \quad r = \pi_j^{\psi} - \pi_i^{\psi} + q_{ij}^{\psi} T, \quad h\delta = \eta_{ijt}^{\psi}, \\ 0 & \text{otherwise.} \end{cases} \tag{24}$$

where $(i, j) \in A_{\text{run}}^{\psi}, t \in \Omega$. The total power consumption at timestamp t, denoted by w_t^{ψ}, is then calculated as the sum of the power demand of all train runs:

$$w_t^{\psi} = \sum_{\forall (i,j) \in A_{\text{run}}^{\psi}} p_{ijt}^{\psi}, \qquad \forall \quad t \in \Omega. \tag{25}$$

Four different indicators were introduced to evaluate the energy consumption of a given timetable, ψ. In our calculation, $E_{\text{traction}}^{\psi}$ is the traction energy demand, $E_{\text{usedreg}}^{\psi}$ is the regenerative energy immediately used for powering accelerating trains, $E_{\text{restreg}}^{\psi}$ is the remaining regenerative energy (total regenerative energy minus regenerative energy immediately used), and E_{total}^{ψ} is the total energy consumption (traction energy minus regenerative energy) as follows:

$$E_{\text{traction}}^{\psi} = \sum_{\forall t \in \Omega} \sum_{\forall (i,j) \in A_{\text{run}}^{\psi}} \max\{p_{ijt}^{\psi}, 0\}, \tag{26}$$

$$E_{\text{usedreg}}^{\psi} = \sum_{\substack{\forall (i,j),(i',j') \in A_{\text{run}}^{\psi} \\ (i',j) \in A_{\text{sab}}^{\psi}}} \sum_{t = \max\{\pi_{i'}^{\psi}, \pi_j^{\psi} - t_j^{\psi}\}}^{\min\{\pi_j^{\psi}, \pi_{i'}^{\psi} + t_{i'}^{\psi}\}} (\alpha_{i'j}^{\psi} + \beta_{i'j}^{\psi}) \cdot \min\{p_{i'j't}^{\psi}, -p_{ijt}^{\psi}\}, \tag{27}$$

$$E_{\text{restreg}}^{\psi} = \sum_{\forall t \in \Omega} \sum_{\forall (i,j) \in A_{\text{run}}^{\psi}} \max\{-p_{ijt}^{\psi}, 0\} - E_{\text{usedreg}}^{\psi}, \tag{28}$$

$$E_{\text{total}}^{\psi} = \sum_{\forall t \in \Omega} \sum_{\forall (i,j) \in A_{\text{run}}^{\psi}} p_{ijt}^{\psi}. \tag{29}$$

We recall that the energy bill may be determined by the maximum power demand of all trains over a certain interval. We define Δ ($\Delta \ge \delta$) as the time interval, $\Omega_\Delta = [0, \Delta, 2\Delta, \ldots, T - \Delta]$ as the set of discrete timestamps, and $\sigma \in \Omega_\Delta$ as a timestamp within set Ω_Δ. The average power consumption over the time interval $[\sigma, \sigma + \Delta]$ is

$$w_\sigma^{\psi} = \frac{\sum_{t=\sigma}^{\sigma+\Delta} w_t^{\psi}}{\Delta}, \qquad \forall \sigma \in \Omega_\Delta. \tag{30}$$

C. Power Peak Shaving Algorithm

Algorithm 1 is designed to explore the optimal solutions of the timetable adjustment model presented in Section III and to enhance the extent to which power peak shaving benefits from the optimized timetables. In Algorithm 1, ψ^* represents the local optimal timetable in terms of the minimal power peak, J^* is equal to the value of the optimized overlapping time obtained by solving the timetable adjustment model, C represents the computational time, $C^{\max}$ is the maximum allowed computational time, I is the number of iterations, $I^{\max}$ is the maximum allowed number of iterations, and W_σ^{ψ} is the locally determined minimum power peak value. The initial value of W_σ^{ψ} was set to ∞.

In each iteration of Algorithm 1, Steps 1 and 2 (S1 and S2) adopt a newly generated objective function (J_2) and aim to find a timetable subject to constraints (1–5, 9–21), and $\sum_{(i,j) \in A_{\text{sab}}} L_{ij} = J^*$. The optimized timetable is denoted by ψ^{new}. The optimized timetable is equivalent to an optimal solution of the timetable adjustment model because its overlapping time is equal to the minimum overlapping time ($\sum_{(i,j) \in A_{\text{sab}}} L_{ij} = J^*$). Algorithm 1 uses different objective functions in each iterative cycle, such that the optimal solutions obtained in different cycles are different. Thus, more feasible solutions subject to constraints (1–5, 9–21), and $\sum_{(i,j) \in A_{\text{sab}}} L_{ij} = J^*$ are explored. These solutions are compared in Step 3 (S3) to find the local optimal timetable in terms of the minimal power peak; if the timetable obtained from S1 and S2 has a smaller power peak value ($w_\sigma^{\psi^{\text{new}}}$) than W_σ^{ψ}, S3 updates the local optimal timetable with $\psi^* = \psi^{\text{new}}$, and updates the value of W_σ^{ψ} with $W_\sigma^{\psi} = w_\sigma^{\psi^{\text{new}}}$. Step 4 (S4) determines whether the computational time and number of iterations exceed the maximum allowed values, and accordingly terminate the algorithm, or loop back to Step 1.

V. Evaluate Synchronization and Robustness Under Delay Circumstances

In real operations, the optimized timetable might not be effectively adhered to, if the train operations are disrupted by unexpected delays. The first priority of trains that were delayed is to resume their original schedule, instead of forcing synchronized acceleration and braking processes. This might detrimentally affect their power consumption. This leads to the following research question: is the optimized timetable

Algorithm 1 An Iterated Local Search Algorithm for Power Peak Shaving

Input: $C = 0$, $I = 0$, $C^{\max}$, $I^{\max}$, $W_\sigma^\psi = \infty$
Output: a local optimal timetable ψ^*
while $C < C^{\max}$, $I < I^{\max}$ **do**
S1: generate a new objective function $J_2 = B \cdot \Pi$, where Π is an $N \times 1$ vector which contains the arrival/departure times of all events (N represents the number of all arrival/departure events.). B is a $1 \times N$ vector of random numbers whose elements are normally distributed with mean 0, variance 1, and standard deviation 1.
S2: solve the following model and obtain a new timetable ψ^{new}:

$$\begin{aligned} \min \quad & J_2 = B \cdot \Pi, \\ s.t. \quad & \sum_{(i,j)\in A_{\text{sab}}} L_{ij} = J^*, \\ & \text{Constraints } (1-5,\ 9-21), \end{aligned}$$

where J^* refers to the optimal solution by solving the timetable adjustment model in Section III.[1]
S3: compute the power peak value of timetable ψ^{new} ($w_\sigma^{\psi^{\text{new}}}$) with Equation (30).
if $w_\sigma^{\psi^{\text{new}}} \le W_\sigma^\psi$ **then**
update the local optimal timetable ψ^*: $\psi^* = \psi^{\text{new}}$;
update W_σ^ψ: $W_\sigma^\psi = w_\sigma^{\psi^{\text{new}}}$.
end
S4: update C and I ($I = I + 1$).
end

vulnerable to delays, which would decrease the potential decrease in energy consumption and power-peak shaving?

To answer this question, we built a model to enable us to use Monte Carlo simulation to evaluate the timetable in terms of robustness against delays, usage of regenerative energy, and power peaks in the case of delays. The Monte Carlo simulation follows an iterative approach, with random entrance delays generated in each iterative cycle. Then, a max-plus-based method [31] was used to simulate the propagation of delays over time periods. This method is able to quickly estimate the departure and arrival times of trains under delay circumstances using max-plus algebra. Based on the estimated departure and arrival times, we compute the number of delay-affected periods (i.e., the time periods until delays fade out are defined as delay-affected time periods; the smaller the number of delay-affected periods, the less severe the effect of delay propagation is), the number of delayed events, and the average delay in one time period (i.e., the sum of delays of all events divided by the number of time periods affected by delays). These three values are adopted to indicate the robustness of the tested timetable against delay propagation. In addition, we computed the average overlapping times of acceleration and braking processes in one time period (i.e., total overlapping times within delay-affected time periods divided by the number of delay-affected time periods), the average energy consumption in one time period (i.e., total energy consumption within delay-affected time periods divided by the number of delay-affected time periods), and the power peaks ($\Delta = 1$ s, 15 min) within delay-affected time periods, to evaluate the energy efficiency of the tested timetable.

[1]Modern commercial solvers (like Gurobi) allow users to perform optimization with multiple/hierarchical objectives. The solutions pools can be used to obtain solution variations.

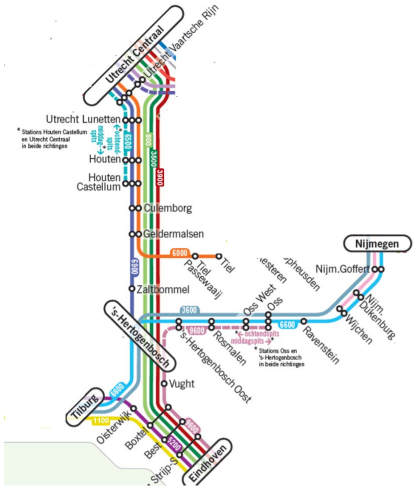

Fig. 2. Train services between Ut and Ehv.

VI. Case Study

A. Setup

We conducted a case study by applying the approach to a central section of the railway network in the Netherlands, bounded by the five main stations of Utrecht (Ut), Eindhoven (Ehv), Tilburg (Tb), and Nijmegen (Nm), and 's-Hertogenbosch (Ht), plus 20 additional smaller stations and stops. A map of this network is shown in Fig. 2.

Overall, 40 trains per hour ran on this network. The timetable adjustment model settings were determined by repeating the timetable every half hour, which means the time period was $T = 30$ min. The timetable in this study was defined to the nearest 6 seconds (for example, a train departs from Ht station at 26.3 minutes past eight and arrives at 48.6 minutes past eight, where 26.3 and 48.6 minutes are both integer multiples of 6 s). To build the timetable adjustment model as an MILP model, we scaled the period time T by $T = 30 \times 10 = 300$, and re-scaled the optimized results by dividing event times by 10. The lower bounds of the running times are equal to the technical minimum running times. The maximum running times are set as 1.05 times the running times used in the original timetable. The minimum dwell time for regional trains at small stations is 0.5 minutes. At other stations, the minimum dwell time was 2 min. The minimum headway time between two arrival events, two departure events, or one arrival and one departure event was 3 min. The minimum headway time between a passing event and an arrival/departure/passing event was 2 min. The minimum turnaround time was 6 min, and the maximum was 20 min. The minimum transfer time

was 3 min, and the maximum was 10 min. The adjustment model allows 3 minutes shifting in arrival/departure event times by setting $c_{\min} = -3$ min and $c_{\max} = 3$ min. The case study includes time allowances in running time and headway time activities as mandatory. Here, for every running time activity $(i, j) \in A_{\text{run}}$, χ_{ij} in Equation (21) is set as 5% of the technical minimum running times. For every headway time activity $(i, j) \in A_{\text{headway}}$, χ_{ij} is set to 6 s (the smallest time unit). Moreover, we focus on the synchronization pairs within one station, instead of one electrical section, as we do not have information on the location of power substations. In other words, all event pairs within A_{sab} are the arrival and departure events of different trains at the same station.

B. Impacts of Different Levels of Robustness

First, we optimize the timetable to improve the time during which synchronized acceleration and braking processes overlap by using the model presented in Section III. This model aims to maximize the objective functions (8) subject to constraints (1-5 and 9–21). The model contains an ε constraint (Equation (20)) to maintain timetable robustness. We use three different sets of weight factors to compute the robustness level θ to understand the impact of weight factors on our optimization results. The three respective sets are: (A) $\gamma_1 = 0.25, \gamma_2 = 0.25, \gamma_3 = 0.5$; (B) $\gamma_1 = 0.33, \gamma_2 = 0.33, \gamma_3 = 0.33$; and (C) $\gamma_1 = 0.5, \gamma_2 = 0.25, \gamma_3 = 0.25$. For each set, the sum of the three weights is 1. Different sets place different importance on running time allowances, dwell time allowances, and headway allowances. To determine an appropriate value for ε in Equation (20) for each set of weight factors, we first aim to find two extreme points, the minimum/maximum robustness level by maximizing or minimizing the total weighted time allowance (θ) subject to constraints (1–5, 19, and 21). With the minimum and maximum values of θ, we select ten values of ε equally spaced between the maximum and minimum values of θ. Then, the model (i.e., objective (8) subject to constraints (1-5 and 9–21)) is solved for these ten different values of ε in Equation (20).

The results are presented in Fig. 3. On the left, the black dots represent the optimized overlapping times, which are obtained by solving the timetable adjustment model with three different sets of weight factors and different values of ε. On the right, the black dots show the optimized time allowances versus the optimized overlapping times. The blue dots indicate the total weighted time allowances and overlapping times using the original timetable. The weighted time allowances of the original timetable were computed using three different weight factor sets.

Overall, the three weight factors that were tested led to similar findings. The overlapping time of the optimized timetable remains at the same high level (1026 s) for small ε values and decreases when the value of ε increases. In Fig. 3 on the right, the optimized timetables (blue dots) have longer overlapping times and greater time allowances than the original timetable (black dots). In summary, the proposed timetable adjustment model improves both the usage of regenerative energy and the robustness of the timetable.

TABLE III
COMPARISON OF THE ORIGINAL AND OPTIMIZED TIMETABLES

KPI	Unit	Original Timetable	Optimized Timetable I
Synchronized pairs	–	10	33
Overlapping time	[s]	258	1026
Traction energy	[10^9 J]	17.13	16.95
Used regenerative energy	[10^9 J]	0.21	0.82
Rest regenerative energy	[10^9 J]	2.04	1.40
Total energy consumption	[10^9 J]	14.89	14.73
CPU time	[s]	–	12.48

C. Optimized Timetable

Subsequently, without loss of generality, we chose one set of weight factors, $\gamma_1 = 0.33, \gamma_2 = 0.33, \gamma_3 = 0.33$ (which emphasizes the running time, dwell time, and headway time allowances to an equal extent), and one robustness level of $\varepsilon = 376.2$ min (the total weighted time allowance with the original timetable is equal to 376.2 min), for which we present the optimized results in this section. As an illustration of our results, we present the optimized timetable for the corridor Utrecht–Eindhoven (with train services 800, 3500, 3900, 6000, and 6900) in Fig. 5. Fig. 4 shows the original timetable of the corridor Utrecht–Eindhoven for comparison. The time-distance diagrams are based on the timetables used in 2019. In Fig. 4 and 5, the intercity services and regional trains are presented in blue and red, respectively. The green circles indicate the synchronized acceleration and braking pairs.

The optimized results for the entire network are reported in Table III, in which a set of key performance indicators (KPIs) is introduced to evaluate the original and optimized timetables. The terms "synchronized pairs" and "overlapping time", respectively, refer to the total number and overlapping time of the synchronized pairs. The "traction energy" ($E^{\psi}_{\text{traction}}$) refers to the sum of the traction energy of all trains, the "used regenerative energy" ($E^{\psi}_{\text{usedreg}}$) is the regenerative energy directly used for accelerating trains, the "rest regenerative energy" ($E^{\psi}_{\text{restreg}}$) is the regenerative energy that is not used for accelerating trains, and the "total energy consumption" (E^{ψ}_{total}) is equal to the total traction energy minus the total regenerative energy. $E^{\psi}_{\text{traction}} \sim E^{\psi}_{\text{total}}$ are computed using Equations (26-29). The "CPU time" refers to the computation time required to solve the timetable adjustment model.

The results show that using the proposed timetable adjustment method increases the number of synchronized pairs. Taking the corridor between Ut and Ehv in Fig. 4 and 5 for example, the original timetable only contains five synchronized pairs whereas the optimized timetable contains thirteen pairs. As a result of the increased synchronized pairs, the overlapping time increases by 297%, and the regenerative energy usage increases by 290% for the entire network. The optimized timetable consumes less traction energy than the original timetable (1.06% less). The optimized timetable prescribes 2 min more running time than the original timetable (762.5 versus 760.5 minutes), which is the reason for the lower traction energy of the optimized timetable. The optimized timetable has a specified maximum running time 1.05 times

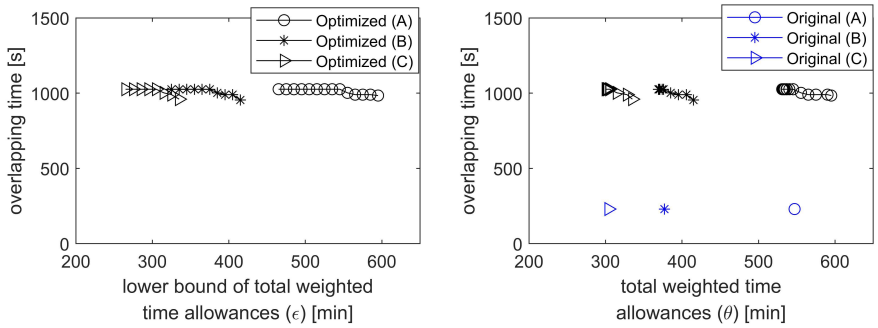

Fig. 3. Overlapping times for different values of ε.

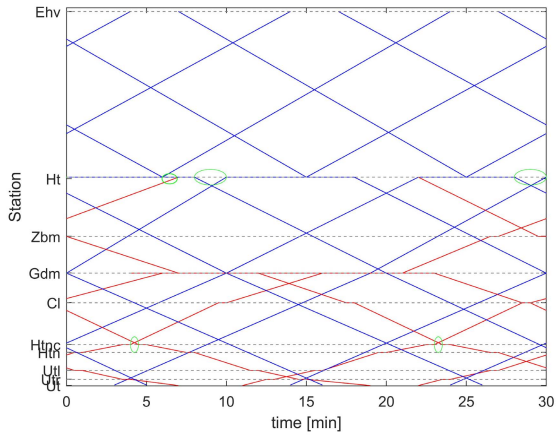

Fig. 4. Original timetable.

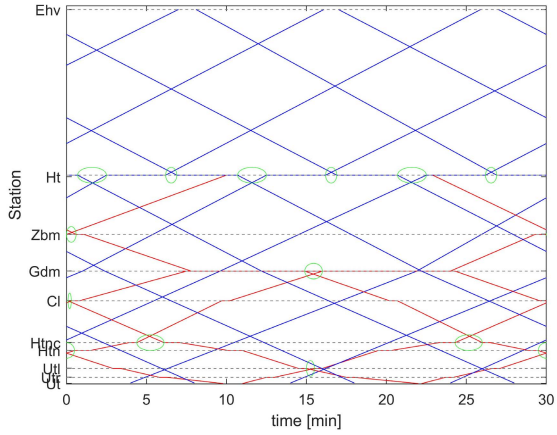

Fig. 5. Optimized timetable.

that of the original timetable, to allow the model the necessary flexibility with which to adjust the running time without affecting the corridor capacity.

D. Power Peak Shaving

In this section, the power peak shaving algorithm (Algorithm 1) is examined. The maximum computational time is specified as $C^{\max} = 10$ h, and the maximum number of iterations as $I^{\max} = 1000$. We set $\delta = 1$ s and created a

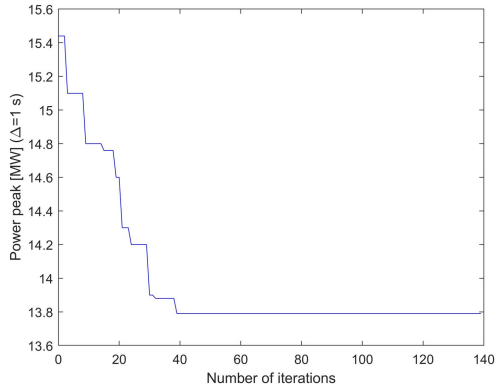

Fig. 6. Convergence curve.

representative power profile for every train run depending on the type of train, run time, speed limits, and gradients using the MPOC method [33]. The convergence curve in Fig. 6 shows that the power peak values ($\Delta = 1$ s) converge at the 38-th iterative cycle.

Fig. 7 compares the power profiles of the original and optimized timetables. The timetable obtained in Section VI-C is referred to as "optimized timetable I", and the timetable obtained by running the power peak shaving algorithm is referred to as "optimized timetable II". The power profiles are reported for different intervals (Δ of 1 s, 1 min, 5 min, and 15 min). The numerical results are reported in Table IV. In Fig. 7, the power peaks of optimized timetable II are the lowest. The 1-second, 1-minute, 5-minute, and 15-minute power peaks of optimized timetable II are reduced by 25.1%, 17.8%, 15.6%, and 8.5%, respectively, compared with the original timetable. These results show that the timetable adjustment model and the power peak shaving method contribute to the reduction of the power peaks. Moreover, the power peaks of timetable II are lower than those of timetable I (the blue lines are below the green lines in Fig. 7), meaning the power peak shaving algorithm enhances the benefit of using regenerative energy in power peak shaving.

E. Impact of Delays

We next examined the extent to which the original timetable and optimized timetable II adapt to delays by performing Monte Carlo simulations using the max-plus theory.

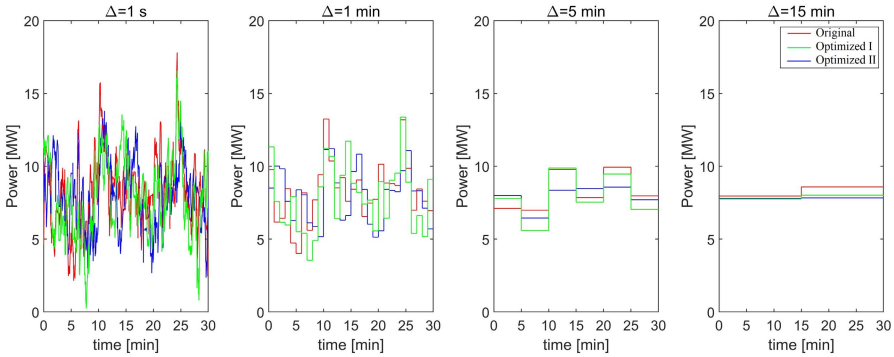

Fig. 7. Power profiles using the original timetable and optimized timetables I and II.

TABLE IV
COMPARISON OF POWER PEAKS

Power peak	Unit	Original Timetable	Optimized Timetable I	Optimized Timetable II
$\Delta =$ 1 s	[MW]	18.41	16.48	13.79
$\Delta =$ 1 min	[MW]	13.63	13.38	11.21
$\Delta =$ 5 min	[MW]	10.18	9.88	8.59
$\Delta =$ 15 min	[MW]	8.58	8.01	7.83

TABLE V
ESTIMATED IMPACT OF DELAYS

KPI	Unit	Original Timetable	Optimized Timetable II
Number of affected periods	–	3.74	3.10
Number of affected events	–	234.92	220.42
Overlapping time	[s]	295.78	654.01
Energy consumption	[10^9 J]	15.01	14.91
Power peak (Δ=1 sec)	[MW]	18.43	16.41
Power peak (Δ=15 min)	[MW]	9.43	9.38

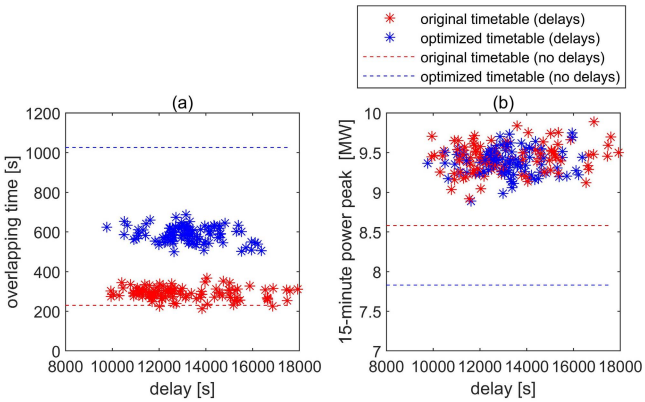

Fig. 8. Numerical estimation of the impact of delays.

We first generated 100 random entrance delays based on a three-parameter Weibull distribution. This distribution has also been used in other research pertaining to railway optimization [34], [35]. In this study, we assumed two different distributions for intercity (ICs) and local trains (SPs). The scale, shape, and shift parameters were 394, 2.27, and 315 for the ICs and 470, 3, and 186 for the local trains, respectively. Second, 100 random delays were taken as the entrance delays of trains in a time period to generate 100 delay situations. For each case, the max-plus-based method described in Section V was adopted to estimate the delay propagation through that time period and successive time periods until the delay is eliminated, assuming train operations are guided by either the original or the optimized timetable. At the same time, the utilization of the regenerative energy and power peaks of the 100 cases were examined as well.

The simulation results are presented in Table V, which reports the average values of the 100 cases, and Fig. 8. The definitions of the KPIs in the first column are provided in Section V. Fig. 8 displays the simulation results of all 100 delay cases. The simulation results of the original and optimized timetables are presented in red and blue dots/lines, respectively.

The optimized timetable requires less time to recover from delays than the original timetable (3.10 $<$ 3.74). The number of affected events and average delays with the optimized timetable are also smaller than those with the original timetable. In other words, the optimized timetable is more robust against delays compared with the original timetable. This is explained by the fact that the optimized timetable is obtained with constraints (19–21). Constraints (19–20) ensure the overall robustness of the timetable, whereas constraint (21) guarantees that a minimum time allowance is included in every running/dwell/headway activity. The lower bound of Equation (20) is set to be 376.2 min, which is equal to the total weighted time allowance of the original timetable. This means that the overall time allowances of the optimized timetable are equal to or higher than the time allowances of the original timetable. These settings enhance the robustness of the optimized timetable.

The simulation results also showed that delays affect the usage of regenerative energy. The overlapping time of acceleration and braking processes, using the optimized timetable is reduced from the theoretical 1026 s to 654.01 s, whereas the overlapping time, using the original timetable is increased from the theoretical 258 s to 295.78 s. This means that the optimized timetable cannot achieve its theoretical usage of regenerative energy when delays occur, whereas the original

timetable might be superior in terms of making use of regenerative energy when delays occur than under normal (on-time) circumstances. This can be understood by considering that the optimized timetable was computed by maximizing the overlapping time without considering delays or disruptions. Delayed arrivals and departures disrupt the designed acceleration and braking synchronizations, and therefore affect the usage of regenerative energy. The original timetable, instead, does not initially have many synchronized pairs (10 pairs only). Late arrivals and departures can improve synchronizations. However, as shown in Fig. 8 (a), the optimized timetable still outperforms the original timetable in terms of overlapping times. In other words, the optimized timetable still enables more efficient regenerative energy consumption than the original timetable, even when delays are taken into consideration.

We additionally examined the extent to which delays affect the 1-second and 15-minute power peaks. The simulation results show that the use of the optimized timetable increases the 1-second and 15-minute power peaks from the theoretical 13.79 MW to 16.41 MW, and from 7.83 MW to 9.38 MW, respectively. This increase is expected because delayed trains run faster (less running time) to recover from delays and restore their schedules, such that the demand for traction energy is increased under delayed circumstances. Moreover, as discussed above, delays cause a reduction in the consumption of regenerative energy, which also contributes to the increase in power peaks. Similarly, delays increase the average 1-second and 15-minute power peaks when the original timetable is used.

In summary, the Monte Carlo simulation suggests that although the optimized timetable cannot achieve its theoretical ability to use regenerative energy and power peak shaving for the delays that were tested, the optimized timetable outperforms the original timetable in terms of delay recovery, energy efficiency, and power peak shaving.

VII. Conclusion

In this study, we aimed to fine-tune the timetable to optimize the utilization of regenerative energy and shaving power peaks. An MILP model was formulated for timetable adjustment. The model was designed to increase the overlap between the synchronized acceleration and braking of trains to optimize the consumption of regenerative energy. The model has built-in restrictions on time allowances to ensure that the timetable robustness is maintained at a required level. A power peak shaving algorithm was developed to optimize the timetable in terms of power peak shaving. To examine the extent to which the original and optimized timetables were able to adapt to unplanned delays, Monte Carlo simulation was used to evaluate the robustness and energy efficiency of the timetables during delays. Using the proposed models, a case study was designed to fine-tune the 2019 timetable for a subnetwork of the Dutch railway network. The results showed that the optimized timetable outperforms the original timetable in terms of timetable robustness, utilization of regenerative energy, and shaving power peaks under both on-time and delayed circumstances.

The proposed model is suitable for fine-tuning timetables of the Dutch railway network, as well as similar periodic timetables used in other regions (along corridors with high frequency, dense traffic, and balanced traffic flows). Although this case study focused on synchronizing events within the same station, it could be extended to synchronize events within one electrical section. In this case, utilization of the regenerative energy and lower power peaks would be expected to improve. Moreover, the proposed method could be extended to AC situations and electric vehicles in general such as underground metropolitan trains or trams.

Furthermore, despite its successful outcome, this study has certain limitations. First, the proposed model focuses on increasing the amount of synchronized acceleration and braking pairs, assuming that one braking process corresponds to exactly one acceleration process. This is highly applicable to the operations along corridors that carry high frequency and dense traffic, and balanced traffic flows. The model would have to be extended considering that one braking process might correspond to more than one acceleration process. Optimization of the distribution of the cumulative braking energy of multiple braking trains over multiple accelerating trains, and embedding this in a network timetable optimization problem would require further research. Second, the electrical system was not considered in this work. However, to move towards practical implementation and to smooth the power voltage in the planning phase, it is necessary to consider the restrictions of the power system, either by reflecting the power system characteristics in the timetable design phase or by examining the optimized results while considering the power flows of the electrical system.

References

[1] T. Albrecht, "Reducing power peaks and energy consumption in rail transit systems by simultaneous train running time control," *WIT Trans. State Art Sci. Eng.*, vol. 39, pp. 1–10, Mar. 2010.

[2] A. Bärmann, P. Gemander, A. Martin, M. Merkert, and F. Nöth, "Energy-efficient timetabling in a German underground system," Dept. Math., Friedrich-Alexander-Universität Erlangen-Nürnberg, Erlangen, Germany, Tech. Rep., 2018.

[3] M. Khodaparastan, A. A. Mohamed, and W. Brandauer, "Recuperation of regenerative braking energy in electric rail transit systems," *IEEE Trans. Intell. Transp. Syst.*, vol. 20, no. 8, pp. 2831–2847, Aug. 2019.

[4] X. Yang, X. Li, B. Ning, and T. Tang, "A survey on energy-efficient train operation for urban rail transit," *IEEE Trans. Intell. Transp. Syst.*, vol. 17, no. 1, pp. 2–13, Jan. 2015.

[5] G. M. Scheepmaker, R. M. Goverde, and L. G. Kroon, "Review of energy-efficient train control and timetabling," *Eur. J. Oper. Res.*, vol. 257, no. 2, pp. 355–376, 2017.

[6] C. S. Chang, Y. H. Phoa, W. Wang, and B. S. Thia, "Economy/regularity fuzzy-logic control of DC railway systems using event-driven approach," *IEE Proc., Electr. Power Appl.*, vol. 143, no. 1, pp. 9–17, 1996.

[7] A. Ramos, M. T. Pena, A. Fernández, and P. Cucala, "Mathematical programming approach to underground timetabling problem for maximizing time synchronization," *Dirección Organización*, no. 35, pp. 88–95, Jun. 2008.

[8] M. Peña-Alcaraz, A. Fernández, A. P. Cucala, A. Ramos, and R. R. Pecharromán, "Optimal underground timetable design based on power flow for maximizing the use of regenerative-braking energy," *Proc. Inst. Mech. Eng. F, J. Rail Rapid Transit*, vol. 226, no. 4, pp. 397–408, 2011.

[9] X. Yang, X. Li, Z. Gao, H. Wang, and T. Tang, "A cooperative scheduling model for timetable optimization in subway systems," *IEEE Trans. Intell. Transp. Syst.*, vol. 14, no. 1, pp. 438–447, Mar. 2013.

[10] X. Li and X. Yang, "A stochastic timetable optimization model in subway systems," *Int. J. Uncertainty Fuzziness Knowl.-Based Syst.*, vol. 21, no. 1, pp. 1–15, Jul. 2013.

[11] X. Yang, A. Chen, X. Li, B. Ning, and T. Tang, "An energy-efficient scheduling approach to improve the utilization of regenerative energy for metro systems," *Transp. Res. C, Emerg. Technol.*, vol. 57, pp. 13–29, Aug. 2015.
[12] H. Liu, M. Zhou, X. Guo, Z. Zhang, N. Bin, and T. Tang, "Timetable optimization for regenerative energy utilization in subway systems," *IEEE Trans. Intell. Transp. Syst.*, vol. 20, no. 9, pp. 3247–3257, Sep. 2019.
[13] H. Sun, J. Wu, H. Ma, X. Yang, and Z. Gao, "A bi-objective timetable optimization model for urban rail transit based on the time-dependent passenger volume," *IEEE Trans. Intell. Transp. Syst.*, vol. 20, no. 2, pp. 604–615, Feb. 2019.
[14] A. Bärmann, A. Martin, and O. Schneider, "A comparison of performance metrics for balancing the power consumption of trains in a railway network by slight timetable adaptation," *Public Transp.*, vol. 9, nos. 1–2, pp. 95–113, Jul. 2017.
[15] Y. Bai, Y. Cao, Z. Yu, T. K. Ho, C. Roberts, and B. Mao, "Cooperative control of metro trains to minimize net energy consumption," *IEEE Trans. Intell. Transp. Syst.*, vol. 21, no. 5, pp. 2063–2077, May 2020.
[16] X. Sun, H. Cai, X. Hou, M. Zhang, and H. Dong, "Regenerative braking energy utilization by multi train cooperation," in *Proc. 17th Int. IEEE Conf. Intell. Transp. Syst. (ITSC)*, Oct. 2014, pp. 139–144.
[17] J. Liu, H. Guo, and Y. Yu, "Research on the cooperative train control strategy to reduce energy consumption," *IEEE Trans. Intell. Transp. Syst.*, vol. 18, no. 5, pp. 1134–1142, May 2017.
[18] S. Su, T. Tang, X. Li, and Z. Gao, "Optimization of multitrain operations in a subway system," *IEEE Trans. Intell. Transp. Syst.*, vol. 15, no. 2, pp. 673–684, Apr. 2014.
[19] S. Su, T. Tang, and C. Roberts, "A cooperative train control model for energy saving," *IEEE Trans. Intell. Transp. Syst.*, vol. 16, no. 2, pp. 622–631, Apr. 2014.
[20] S. Su, X. Wang, Y. Cao, and J. Yin, "An energy-efficient train operation approach by integrating the metro timetabling and eco-driving," *IEEE Trans. Intell. Transp. Syst.*, vol. 21, no. 10, pp. 4252–4268, Oct. 2020.
[21] X. Li and H. K. Lo, "An energy-efficient scheduling and speed control approach for metro rail operations," *Transp. Res. B, Methodol.*, vol. 64, pp. 73–89, Jun. 2014.
[22] X. Li and H. K. Lo, "Energy minimization in dynamic train scheduling and control for metro rail operations," *Transp. Res. B, Methodol.*, vol. 70, pp. 269–284, Dec. 2014.
[23] X. Yang, B. Ning, X. Li, and T. Tang, "A two-objective timetable optimization model in subway systems," *IEEE Trans. Intell. Transp. Syst.*, vol. 15, no. 5, pp. 1913–1921, Oct. 2014.
[24] L. S. Zhou, L. Tong, J. Chen, J. Tang, and X. Zhou, "Joint optimization of high-speed train timetables and speed profiles: A unified modeling approach using space-time-speed grid networks," *Transp. Res. B, Methodol.*, vol. 97, pp. 157–181, Mar. 2017.
[25] Y. Xu, B. Jia, X. Li, M. Li, and A. Ghiasi, "An integrated micro-macro approach for high-speed railway energy-efficient timetabling problem," *Transp. Res. C, Emerg. Technol.*, vol. 112, pp. 88–115, Mar. 2020.
[26] S. Lu, P. Weston, S. Hillmansen, H. B. Gooi, and C. Roberts, "Increasing the regenerative braking energy for railway vehicles," *IEEE Trans. Intell. Transp. Syst.*, vol. 15, no. 6, pp. 2506–2515, Dec. 2014.
[27] P. Wang and R. M. P. Goverde, "Multi-train trajectory optimization for energy-efficient timetabling," *Eur. J. Oper. Res.*, vol. 272, no. 2, pp. 621–635, 2019.
[28] P. Serafini and W. Ukovich, "A mathematical model for periodic scheduling problems," *SIAM J. Discrete Math.*, vol. 2, no. 4, pp. 550–581, Nov. 1989.
[29] E. V. Andersson, A. Peterson, and J. T. Krasemann, "Quantifying railway timetable robustness in critical points," *J. Rail Transp. Planning Manage.*, vol. 3, no. 3, pp. 95–110, Aug. 2013.
[30] F. Yan, N. Bešinović, and R. M. P. Goverde, "Multi-objective periodic railway timetabling on dense heterogeneous railway corridors," *Transp. Res. B, Methodol.*, vol. 125, pp. 52–75, Jul. 2019.
[31] R. M. P. Goverde, "Railway timetable stability analysis using max-plus system theory," *Transp. Res. B, Methodol.*, vol. 41, no. 2, pp. 179–201, Feb. 2007.
[32] X. Zhang and L. Nie, "Integrating capacity analysis with high-speed railway timetabling: A minimum cycle time calculation model with flexible overtaking constraints and intelligent enumeration," *Transp. Res. C, Emerg. Technol.*, vol. 68, pp. 509–531, Jul. 2016.
[33] P. Wang and R. M. P. Goverde, "Multiple-phase train trajectory optimization with signalling and operational constraints," *Transp. Res. C, Emerg. Technol.*, vol. 69, pp. 255–275, Aug. 2016.
[34] E. Quaglietta, F. Corman, and R. M. P. Goverde, "Stability analysis of railway dispatching plans in a stochastic and dynamic environment," *J. Rail Transp. Planning Manage.*, vol. 3, no. 4, pp. 137–149, Nov. 2013.
[35] F. Corman and E. Quaglietta, "Closing the loop in real-time railway control: Framework design and impacts on operations," *Transp. Res. C, Emerg. Technol.*, vol. 54, pp. 15–39, May 2015.

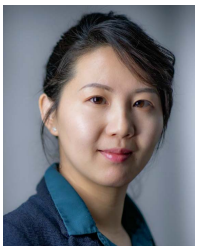

Pengling Wang received the B.Sc. degree from Southwest Jiaotong University, China, in 2011, and the Ph.D. degree jointly from Southwest Jiaotong University and the Delft University of Technology, The Netherlands, in 2017. She is currently an Assistant Professor at Tongji University. Her research interests include rail traffic management and energy-efficient train driving.

Nikola Bešinović was born in Serbia, in 1985. He received the B.Sc. and M.Sc. degrees from the University of Belgrade, Serbia, and the Ph.D. degree in transport from the Delft University of Technology, The Netherlands. He is currently a Lecturer and a Researcher at the Department of Transport and Planning, Delft University of Technology. His main research interests include optimization and AI in railway and public transport systems.

Rob M. P. Goverde (Member, IEEE) is currently a Professor of railway traffic management and operations and the Director of the Digital Rail Traffic Laboratory, Delft University of Technology, The Netherlands. He chairs the railway systems theme of the TU Delft Transport Institute. His expertizes include operations research, optimal control, max-plus algebra, and data analytics applied to railway traffic and transport. He is the President of the International Association of Railway Operations Research (IAROR) and a fellow of the Institution of Railway Signal Engineers (FIRSE). He is the Editor-in-Chief of the *Journal of Rail Transport Planning and Management* and an Associate Editor of IEEE TRANSACTIONS ON INTELLIGENT TRANSPORTATION SYSTEMS.

Francesco Corman (Member, IEEE) was born in Italy, in 1982. He received the Ph.D. degree in transport sciences from TU Delft, The Netherlands, on operations research techniques for real-time railway traffic control. Since 2017, he has been the Chair of transport systems at the Institute of Transport Planning and Systems, ETH Zürich. His main research interests are in the application of quantitative methods and operations research to transport sciences, especially railway operations and logistics.